A DDX31/mutant-p53/EGFR axis promotes multistep progression of muscle invasive bladder cancer

Kei Daizumoto[1,2], Tetsuro Yoshimaru[1], Yosuke Matsushita[1], Tomoya Fukawa[1,2], Hisanori Uehara[3], Masaya Ono[4], Masato Komatsu[1], Hiro-omi Kanayama[2], and Toyomasa Katagiri[1]

[1]Division of Genome Medicine, Institute for Genome Research, Tokushima University, Tokushima, Japan; [2]The Department of Urology, Institute of Biomedical Sciences, Tokushima University Graduate School, Tokushima, Japan; [3]Division of Pathology, Tokushima University Hospital, Tokushima, Japan; [4] Department of Clinical Proteomics, National Cancer Center Research Institute, Tokyo, Japan.

Running title: Critical roles of DDX31-mutp53-EGFR axis in MIBC progression

Corresponding Author: Toyomasa Katagiri, Division of Genome Medicine, Institute for Genome Research, Tokushima University, 3-18-15, Kuramoto-cho, Tokushima 770-8503, Japan. Phone: 81-88-633-9477; Fax: 81-88-633-7989; E-mail: tkatagi@genome.tokushima-u.ac.jp

Disclosure of Potential Conflicts of Interest: No potential conflicts of interest were disclosed.

ABSTRACT

The p53 and EGFR pathways are frequently altered in bladder cancers, yet their contributions to its progression remain elusive. Here we report that DEAD box polypeptide 31 (DDX31) plays a critical role in the multistep progression of muscle invasive bladder cancer (MIBC) through its sequential interactions with mutant p53 (mutp53) and EGFR. In early MIBC cells, nuclear DDX31 bound mutp53/SP1 and enhanced mutp53 transcriptional activation, leading to migration and invasion of MIBC. Cytoplasmic DDX31 also bound EGFR and phospho-nucleolin (p-NCL) in advanced MIBC, leading to EGFR-Akt signaling activation. High expression of both cytoplasmic DDX31 and p53 proteins correlated with poor prognosis in patients with MIBC, and blocking the DDX31-NCL interaction resulted in downregulation of EGFR-Akt signaling, eliciting an *in vivo* anti-tumor effect against bladder cancer. These findings reveal that DDX31 cooperates with mutp53 and EGFR to promote progression of MIBC, and inhibition of DDX31-NCL formation may lead to potential treatment strategies for advanced MIBC.

Significance

DDX31 cooperates with mutp53 and EGFR to promote progression of muscle invasive bladder cancer.

INTRODUCTION

Bladder cancer is the most common malignancy of the urinary tract worldwide with approximately 430,000 new cases per year (1). Approximately 70% of cases are diagnosed as non–muscle-invasive bladder cancer (NMIBC), while the remaining 30% of cases are classified as muscle-invasive bladder cancer (MIBC). The standard treatment for MIBC is radical cystectomy, which only provides a five-year survival rate of 50% (2). Cisplatin-containing combination chemotherapy with gemcitabine and cisplatin (GC) or methotrexate, vinblastine, adriamycin and cisplatin (MVAC) is standard treatment for advanced or metastatic bladder cancer patients (3). However, because the overall survival of patients with advanced MIBC remains very poor, a better understanding of the molecular mechanisms of bladder carcinogenesis and progression for the development of new systemic therapies is needed.

Evidence based on molecular biology has highlighted that the aggressiveness of MIBC advances through a multistep mechanism due to many genomic alterations. Notably, *TP53* (which encodes p53 protein) is one of the most frequent genetic lesions in human cancers, especially bladder cancer (4) (5). The majority of *TP53* mutations are caused by missense mutations within

the DNA-binding domain (amino acids 102–292) with hot spots at codons R175, R248, R273 and R282 (6). Mutant p53 proteins (mutp53) lose wild-type p53 (wtp53) transcriptional activity and gain novel oncogenic functions that are independent of wtp53 (7). Accumulating evidence has recently revealed that mutp53 can promote invasion and motility through its activation of transforming growth factor β (TGF-β), epidermal growth factor receptor (EGFR) and MET (8). Moreover, although mutp53 can enhance gene transcription in oncogenic pathways including the mevalonate pathway and the etoposide-resistance pathway via its association with other transcriptional factors such as SREBP (9), ETS2 (10) or prolyl isomerase Pin1 (11), the biological roles of mutp53 gain of function (GOF) in MIBC progression remain unknown.

Furthermore, recent studies have also identified activation of the EGFR pathway in a subgroup of basal-like bladder cancers, which account for 23.5% of MIBC. Its overexpression has also been associated with poor prognoses (12), and MIBC cells with this signature were found to be sensitive to EGFR inhibitors (13). However, the connection between the overexpression of EGFR and the p53 mutation in multistep carcinogenesis and the progression of MIBC remains unknown.

We recently identified DEAD (Asp-Glu-Ala-Asp) box polypeptide 31 (DDX31), a nucleolar protein that is upregulated in the vast majority of human renal cell carcinomas (RCCs). In RCC cells, DDX31 captures nucleophosmin (NPM1) in the nucleoli, which prevents NPM1–HDM2 complex formation in the nucleoplasm and subsequent enhancement of p53 ubiquitination and degradation via the HDM2 pathway, resulting in inactivation of wtp53 protein. This finding proposes a mechanism of wtp53 inactivation in RCC cells that have a low frequency of *TP53* mutations. By contrast, analysis of gene expression profiles (14) revealed that DDX31 is overexpressed in the majority of MIBC, although frequent somatic alterations of the *TP53* gene and EGFR were detected in MIBC cases. Accordingly, we focused on understanding the distinct biological roles of DDX31 in the multi-process progression of MIBC through its association with mutp53 and EGFR.

Here, we show the distinct and crucial roles of nuclear and cytoplasmic DDX31 in the progression of invasive bladder cancer. In the early phase of MIBC, the nuclear DDX31/mutp53 complex promotes invasion and migration by enhancing expression of their target gene, *EPB41L4B*. In the more advanced phase, DDX31 forms a complex with EGFR by interacting with nucleolin (NCL)

under the cytoplasmic membrane of cancer cells, thereby activating the EGFR/Akt signaling pathway. Most importantly, inhibition of the DDX31-NCL interaction promotes an *in vivo* anti-tumor effect in bladder cancer. Thus, the regulation of EGFR-Akt signaling by targeting DDX31-NCL interactions represents a new potential therapeutic target for advanced bladder cancer.

Materials and Methods

Cell lines and specimens

The bladder cancer cell lines RT4, SW780, 5637, J82, T24, UM-UC-3, HT1197, HT1376 and TCCSUP, and normal human urothelial cell line HUC were obtained from the American Type Culture Collection between 2004 and 2015. HEK293 was obtained from RIKEN BRC (Tsukuba, Japan) in 2012. UM-UC-3-GFP was obtained from AntiCancer Japan (Chiba, Japan) in 2011. RT112 was kindly provided by Dr. Osamu Ogawa (Department of Urology, Kyoto University, Kyoto, Japan). HCT116 p53 (+/+) and HCT116 p53 (-/-) were generous gifts from Dr. Bert Vogelstein of Johns Hopkins University. All cells were cultured under conditions recommended by their respective depositors. We monitored the cell morphology of these cell lines using microscopy and

confirmed that they had maintained their morphologic states in comparison with their original morphologic images. No mycoplasma contamination was detected in cultures of any of these cell lines using a Mycoplasma Detection Kit (Roche). Surgically resected bladder tissue samples and their corresponding clinical information were acquired from Tokushima University Hospital (Tokushima, Japan) after obtaining written informed consent. This study was conducted in accordance with the ethical guidelines stated in the Declaration of Helsinki, and approved by the ethical committee of Tokushima University (permission number 28-16). All experiments were conducted according to protocols reviewed and approved by the Committee for Safe Handling of Living Modified Organisms (Permission number 26-40) and the Institutional Animal Care and Use Committee (Permission number 13135) of Tokushima University.

Immunohistochemical staining

Paraffin-embedded tissues were sectioned (6 μm thick) and used to detect the expression of DDX31, p53, EGFR and phospho-Akt (S473) proteins. Immunohistochemical staining was conducted as described previously (15) with anti-DDX31 (1:200), anti-p53 (1:50, DO-7, DAKO A/S, Copenhagen, Denmark),

anti-EGFR (1:50, D38B1, Cell Signaling Technology, Danvers, MA), and anti-phospho-Akt (S473) antibodies (1:50, D9E, Cell Signaling Technology, Danvers, MA). For classification of DDX31 and p53 expression levels, the stained bladder cancer tissues were scored based on a scoring method as follows: the percentage of DDX31-positive cancer cells was scored on a scale of 0 to 4 (0-5%=0 points, 6-25%=1 point, 26-50%=2 points, 51-75%=3 points, 76-100%=4 points). Moreover, the intensity of DDX31 or p53 staining was semi-quantitatively evaluated by the experienced pathologist without prior knowledge of the clinicopathologic data based on the following scoring system: 0: no staining, 1: low staining, 2: moderate staining, and 3: high staining. Cases were accepted as positive only if all evaluators independently defined them as positive. In addition, the product of the DDX31 score (intensity score (0-2 points) × staining area (0-4 points)) was used to divide samples into the following 2 groups (low: 0-3 points; high: 4-8 points), and similarly, the p53 score was used to divide samples into the following 2 groups (low: 0 or 1 points; high: 2 points).

Nuclear/cytoplasmic fractionation

Cytoplasmic fractions including plasma membrane were prepared using the NE-PER nuclear and cytoplasmic extraction reagent (Thermo Fisher Scientific) according to the manufacturer's instructions. β-tubulin and laminin B were used as loading controls for the cytoplasmic and nuclear fractions, respectively.

DDX31–NCL interaction inhibition by DDX31-peptide

The 15 amino-acid peptides derived from the NCL-binding region of DDX31 (codons 750–764) were covalently linked at the NH2-terminus to a membrane transducing the 11 polyarginine sequence (11R) to construct the DDX31 peptide. Control peptides (codons 717-733) were also synthesized (Sigma-Aldrich Japan). To examine the effects of DDX31-peptide on inhibition of DDX31–NCL complex formation, UM-UC-3, UM-UC-3-GFP and J82 cells were treated with 20 μM DDX31-peptide. DDX31–NCL interactions were assessed using co-immunoprecipitation followed by immunoblotting, as described above. To examine the effects of DDX31 peptide on DDX31–NCL-EGFR complex formation, Akt phosphorylation and EGFR protein levels, UM-UC-3-GFP cells

were treated with DDX31-peptide, followed by immunoprecipitation with anti-DDX31 and Western blot with the indicated antibodies.

In vivo tumor growth inhibition

We used BALB/c nude mice (Charles River Laboratories, Tokyo, Japan). All mice were inoculated subcutaneously (s.c.) in the flank with 200 μL (UMUC-3 cells, 1×10^6 cells/mouse) of Dulbecco's phosphate buffered saline (DPBS) with 50% Matrigel (BD Biosciences). The tumors developed over a period of 1 week, reaching sizes of approximately 100 mm^3 [calculated as $1/2 \times (\text{width} \times \text{length}^2)$]. For UM-UC-3 xenograft experiments, the mice were randomized into the following groups (six mice / group): 1) no treatment, 2) PBS (-), 3) DDX31-peptide 3.7 mg/kg, and 4) DDX31-peptide 7.4 mg/kg. DDX31-peptide was delivered via intraperitoneal injection every day, and tumor volumes were measured with calipers for 25 days after the first injection, after which time the animals were killed, and the tumors were excised and frozen in liquid nitrogen. All experiments were performed in accordance with the guidelines of the animal facility at the Tokushima University. For evaluations of the inhibitory effects of DDX31-peptide on tumor, expression of pAkt (S473) and EGFR by

immunohistochemistry. In addition, for evaluations of the effects of DDX31-peptide on the EGFR protein level in tumors, each tumor lysate (six mice per group) was immunoblotted.

Data set for statistical analysis

Publicly available gene expression data sets of TCGA bladder urothelial carcinoma (clinical data, RNAseq expression, mutation, CNV and phosphorylation) were downloaded from the Broad Institute Firehose Pipeline (http://gdac.broadinstitute.org) and the cBioPortal for Cancer Genomics (http://cbioportal.org). The different expression (by fold change value) between bladder cancer tissues and the normal bladder was calculated according to the median gene expression value of each sample.

Kaplan–Meier plot analysis

Overall survival and cancer specific survival curves were estimated using the Kaplan–Meier method. The statistical significance of a relationship between the clinical outcome and gene expression was assessed using the trend log-rank test. We determined a high group, an above median expression

low group, and a bellow median expression as cut-off. Cox proportional hazards analysis was used to identify significant prognostic clinical factors and to test for an independent contribution to overall survival. Statistical significance was calculated using Student's t test to evaluate cell proliferation or gene expression. For the analysis of *in vivo* tumor growth inhibition, Dunnett's test was used to compare the differences between the experimental groups and the control group. A difference of $p<0.05$ was considered statistically significant. * $p<0.05$, ** $p<0.01$ and *** $p<0.005$ were defined. The analysis was performed using SPSS Statistics® 20 (SPSS, IBM Corp, Armonk, NY, USA).

RESULTS

DDX31 overexpression/ mutated *TP53* is involved in the progression of bladder cancer

We verified the significant upregulation of DDX31 in bladder cancer tissues and cell lines at the mRNA and protein levels using the Cancer Genome Atlas (TCGA) dataset (Supplementary Fig. S1A) and Western blot analysis (Supplementary Fig. S1B), respectively. Although a growing number of studies have shown that *TP53* mutations occur frequently in bladder cancer,

Kaplan-Meier analysis using the TCGA bladder cancer cohort dataset showed no significant association between mutated and wild-type *TP53* with respect to overall survival (Supplementary Fig. S1C). Accordingly, we hypothesized that *DDX31* overexpression is involved in the prognosis of bladder cancer patients with *TP53* mutations. Kaplan-Meier analysis showed that bladder cancer patients with both high expression of *DDX31* and mutated *TP53* had significantly shorter overall survival times than patients with low expression of *DDX31* and mutated *TP53* (Fig. 1A, left panel), but high *DDX31* expression and wild-type *TP53* were not significantly associated with a poor prognosis (Fig. 1A, right panel). In addition, we found high frequencies of amplified MDM2 (24%) and deleted CDKN2A (59%) genes in bladder cancer cases with wild-type *TP53* and non-overexpressed *DDX31* by TCGA dataset analysis (Supplementary Fig. S1D).

Furthermore, we performed the univariate and multivariate analyses using stepwise analysis (16) to investigate the impact of DDX31 overexpression versus other genes in the *TP53* mutant population on overall survival of 64 cases with MIBC using TCGA dataset cohort. Univariate analysis showed that *DDX31*, *TP53* and *FN1* were significant correlation with overall survival, but

multivariate analysis showed that only *DDX31* and *TP53* genes were independent predictor of overall survival of MIBC cases (Supplementary Table S1).

To explore the impact of DDX31 on the development and progression of bladder cancer cell lines bearing *TP53* mutations (Supplementary Table S2) and alterations of other cancer-related genes (Supplementary Table S3), we performed invasion, wound healing and spheroid formation assays. A matrigel invasion assay using an xCELLigence system revealed that siRNA-mediated depletion of DDX31 expression led to significant suppression of cell invasion of UM-UC-3 (F113C) and J82 (K320N) cells (Fig. 1B and C), whereas ectopic DDX31 overexpression in TCCSUP (E349X) and HT1376 (P250L) cells, which weakly expressed DDX31, promoted cell invasion (Fig. 1D and E). Next, we confirmed that DDX31 overexpression significantly rescued the reduction of invasion in DDX31-depleted UM-UC-3 and J82 cells (Supplementary Fig. S1E). Subsequent wound healing and spheroid assays revealed that DDX31 silencing significantly decreased cell migration and spheroid formation compared with siEGFP-transfected cells (Supplementary Fig. S1F and G; Fig. 1F and G), indicating that DDX31 promotes cell migration and anchorage-independent

growth. These findings strongly suggest that DDX31 enhances the aggressive behavior of bladder cancer cells bearing *TP53* mutations.

Intriguingly, standard cell proliferation assays revealed that silencing DDX31 expression resulted in reduced cell growth in SW780 cells bearing wild-type *TP53* in a time-dependent manner (Supplementary Fig. S1H and I) but did not in UM-UC-3 and J82 cells with *TP53* mutations (Supplementary Fig. S1J). In addition, ectopic DDX31 overexpression in TCCSUP and HT1376 cells bearing *TP53* mutations also did not affect cell growth (Supplementary Fig. S1K), suggesting that both DDX31 overexpression and *TP53* mutation are required to enhance the progression of bladder cancer cells. As we previously demonstrated that DDX31 regulates the stabilization of wtp53 through its interaction with nucleophosmin (NPM1) and rRNA gene transcription in RCC cells (17), we examined the effect of DDX31 knockdown on the expression level of wtp53 protein in SW780 cells and found that DDX31 depletion caused significant upregulation of wtp53 protein levels (Supplementary Fig. S1L) similar to that in RCC cells (17). By contrast, DDX31 depletion caused no effect on the mtp53 protein level in UM-UC-3 and J82 cells (Supplementary Fig. S1M). Moreover, we confirmed an endogenous DDX31-NPM1 interaction in SW780

cells (Supplementary Fig. S1N), indicating that DDX31 potentially regulates the wtp53 protein level via its interaction with NPM1 in both bladder cancer cells and RCC cells.

Subsequent fluorescence-activating cell sorting (FACS) analysis revealed an increased sub-G1 population at 120 hours after siDDX31 transfection (siEGFP: siDDX31=18.61%: 30.36%; Supplementary Fig. S1O), and Western blot analysis revealed cleaved PARP (Supplementary Fig. S1P). Furthermore, knockdown of DDX31 in SW780 cells significantly reduced the *pre-rRNA* expression (Supplementary Fig. S1Q). These findings suggest that DDX31 overexpression leads to anti-apoptosis via stabilization of wild-type p53 and regulates rRNA gene transcription in bladder cancer cells and RCC cells.

More interestingly, we here demonstrated the interaction of endogenous wtp53 and DDX31 in SW780 cells (Supplementary Fig. S2A), and further identified that the region including TAD2 (transcriptional activation domain 2; 29-61 amino acids) and a part of proline-rich domain (PRD; 61-94 amino acids) of p53 is critical for its interaction with DDX31 (Supplementary Fig. S2B-D). Accordingly, we hypothesized that DDX31 regulates the apoptotic function of wtp53 because the induction of apoptosis was observed in DDX31-depleted

SW780 cells (Supplementary Fig. S1P, Q). Subsequently, we searched the impact of DDX31/wtp53 on the apoptosis-specific p53-target genes (18) by a statistical box plot analysis, and identified the apoptosis-specific p53-target genes, *PUMA* and *Ei24/PIG8* which are expressed higher in bladder cancer cases with low expression of *DDX31* compared to cases with *DDX31* overexpression in the presence of wild-type *TP53* (Supplementary Fig. S2E). On the other hand, there is no significant different expression of genes between high and low expression of *DDX31* under mutated *TP53* status (Supplementary Fig. S2E). Next, we confirmed the up-regulation of *PUMA* and *Ei24/PIG8* genes in *DDX31*-depleted SW780 cells (Supplementary Fig. S2F), suggesting that DDX31 potentially suppress apoptosis induced by *PUMA* and *Ei24/PIG8* genes via its binding to wtp53. Taken together, our findings suggest the possibility that DDX31 potentially stabilize wtp53 protein level via its interaction with NPM1, and also directly binds to wtp53, leading to suppression of apoptosis induced by *PUMA* and *Ei24/PIG8* genes in bladder cancer cells, although the further understanding of mechanism of wtp53 regulation by DDX31 is necessary.

DDX31 interacts with mutp53 and enhances transcription of *EPB41L4B*

Accumulating evidence indicates that GOF of mutp53 contributes to the development and progression of human cancer (19). To understand the involvement of DDX31 in the GOF of mutp53, we examined the ability of DDX31 to interact with endogenous mutp53, which has been reported to result in non-functional transcriptional activity of wtp53, in UM-UC-3 (F113C), J82 (K320N, E271K, V274F) and 5637 (R280T) cells. In these cells, we observed the endogenous DDX31/mutp53 complex via co-immunoprecipitation experiments (Fig. 2A). Subsequently, to search for crucial gene(s) regulated transcriptionally by the DDX31/mutp53 complex, we examined the impact of DDX31/mutp53 on the expression of mutp53 GOF-related genes, including *BUB1, C21orf45, CCNE2, CENPA, CSPF6, DEPDC1, EPB41L4B, FAM64A, NCAPH* and *WDR67* (11). We performed a statistical box-plot analysis using the TCGA cohort dataset to search genes with significantly higher expression in bladder cancer cases with mutated *TP53* than in cases with wild-type *TP53* in the presence of *DDX31* overexpression (high expression) (> median of *DDX31* expression), but with not significantly altered between bladder cancer cases with mutated *TP53* and wild-type *TP53* in the absence of *DDX31* overexpression (low expression) (Supplementary Fig. S3A). Eventually, the *EPB41L4B* (*EHM2*) gene was

identified to be expressed significantly higher in bladder cancer cases with mutated *TP53* compared to cases with wild-type *TP53* in the presence of *DDX31* overexpression (Fig. 2B). However, *EPB41L4B* (*EHM2*) expression was not significantly different between mutated and wild-type *TP53* under low expression of *DDX31* (Fig. 2B), suggesting that *EPB41L4B* is a candidate transcriptional target of the DDX31/mutp53 complex. *EPB41L4B*, a member of the NF2/ERM/4.1 superfamily, was reported to be upregulated in tumor cells with high migratory potential, such as metastatic melanoma, fibrosarcoma, prostate cancer and breast cancer, and to promote cancer progression and metastasis (20, 21). Importantly, Kaplan-Meier analysis revealed that bladder cancer patients with both high expression of *DDX31* and *EPB41L4B* exhibited a significantly poorer prognosis compared to other cases (Fig. 2C). These results suggest the possibility that the DDX31/mutp53 complex upregulates *EPB41L4B*, leading to the aggressive behavior of bladder cancer cells.

We next investigated whether the *EPB41L4B* gene is regulated by the coordinated behavior of DDX31 and mutp53 GOF. It has been reported that the transcriptional regulation by mutp53 requires its complexation with transcriptional factors such as E2F1, VDR, SP1, ETS1 and NF-Y (22). We

searched for consensus binding sites of transcriptional factors within the *EPB41L4B* promoter region using the JASPAR database, an open access database of transcription factor binding profiles (23), and identified a potential SP1-binding site within the *EPB41L4B* promoter region (Supplementary Fig. S3B). Accordingly, we hypothesized that SP1 may be a transcriptional binding partner of the DDX31/mutp53 complex for enhancing transcription of *EPB41L4B*. To test this, we performed co-immunoprecipitation experiments with anti-DDX31 and anti-p53 antibodies using TCCSUP cells, which were stably transfected with DDX31-HA, and found that DDX31-HA formed a complex with endogenous mutp53 and SP1 (Fig. 2D). In addition, we confirmed the endogenous interaction of DDX31-SP1 in HT1197 cells (H365R) (Supplementary Fig. S3C). Subsequently, a ChIP assay was performed using TCCSUP cells overexpressing DDX31-HA. Immunoprecipitation with anti-p53 and anti-DDX31 antibodies confirmed that the DDX31-HA/mutant p53 complex bound to endogenous SP1. Next, a ChIP assay with an anti-p53 antibody indicated binding of the DDX31-HA/mutp53/SP1 complex to genomic fragments including the SP1-binding site (Fig. 2E). Moreover, qRT-PCR results indicated that *EPB41L4B* expression was upregulated in both DDX31-HA and

siEGFP-transfected TCCSUP cells but not in DDX31-HA-transfected or sip53-transfected cells (Fig. 2F), indicating that DDX31/mutp53 can directly activate *EPB41L4B* transcription. In addition, knockdown of mutated *TP53* and *SP1* expressions led to the significant downregulation of *EPB41L4B* expression in UM-UC-3 and J82 cells at 72 and 96 hours after transfection of si*TP53* and si*SP1*, respectively (Supplementary Fig. S3D and E).

Finally, we examined the interaction between DDX31 and hotspot mutp53 (R175H, R248W, R273H and R282W), which are frequently observed in human cancer. We transfected these hotspot mutp53 and DDX31-HA expression vectors into HCT116 p53 (-/-) cells followed by immunoprecipitation with anti-HA-tag or anti-p53 antibodies. The results showed that DDX31-HA formed a complex with all of the hotspot mutp53 and endogenous SP1 proteins (Supplementary Fig. S3F). Subsequent qPCR showed that *EPB41L4B* expression was remarkably upregulated in all cells transfected with both DDX31 and any hotspot mutp53 vectors but was not upregulated in cells transfected with only hotspot mutp53 vectors (Supplementary Fig. S3G). These findings strongly suggest that the DDX31/mutp53/SP1 complex induces upregulation of the *EPB41L4B* gene, leading to bladder cancer progression.

Furthermore, we demonstrated that knockdown of mutated *TP53* led to the significant reduction of invasion in both cell lines and migration in UM-UC-3 cells, respectively (Supplementary Fig. S3H and I). These findings suggest that the gain-of-function activity of mutp53 may be in part involved in the progression behaviors of bladder cancer cells.

Association of DDX31 and p53 positivity with poor prognosis of bladder cancer patients

Mutp53 is stabilized and expressed at high levels in tumors because of an increase in its half-life (22). To examine the relationship between DDX31 expression and p53 expression at the protein level in patients with bladder cancer, we conducted immunohistochemical staining analysis of 77 clinical bladder cancer specimens with the anti-DDX31 antibody, followed by classification of p53 and DDX31 expression levels in the stained tissues based on a scoring method (see Methods; Supplementary Table S4). Both DDX31 and p53 were observed in the nuclei of most of the bladder cancer specimens, although the staining intensities varied across individual cases (Fig. 3A and B). On the other hand, no DDX31 staining was observed in normal bladder tissues

(Supplementary Fig. S4A). We then investigated the correlation between DDX31 and p53 expression in bladder cancer cases with various clinicopathological characteristics. Statistical analysis showed that the pT stage and grade 3 cases were significantly associated with the DDX31 positivity (Supplementary Table S5), whereas there was no difference in p53 expression among any of the characteristics (Supplementary Table S6). Subsequently, we performed univariate and multivariate analyses to determine the indicators of cancer-specific survival. Univariate analysis revealed that, in addition to pT-, N- and M-stages, the combination of DDX31 and p53 scores was a significant predictor of cancer-specific survival (Supplementary Table S7). Multivariate analysis also showed that the pT stage and both DDX31-positive and p53-positive scores were independent predictors of cancer-specific survival (Supplementary Table S7). Kaplan-Meier analysis revealed that bladder cancer patients with high expression of both DDX31 and p53 proteins exhibited a significantly poorer prognosis than patients with low DDX31 expression and high expression of p53 proteins (Fig. 3C), suggesting that DDX31 and p53 expression might be a predictive marker for bladder cancer prognosis.

Interestingly, we noticed that DDX31 was observed in the cytoplasm as well as in the nuclei of cancer cells of MIBC patients with a poor prognosis (Fig. 3D; Supplementary Table S4). To verify the cytoplasmic localization of DDX31 in bladder cancer cells, we performed nuclear/cytoplasmic fractionation of bladder cancer cell lines and observed that DDX31 was expressed in both the nuclei and cytoplasm of all bladder cancer cell lines (Supplementary Fig. S4B), although the nuclear/cytoplasmic expression pattern of DDX31 was not dependent on p53 mutation status (Supplementary Table S4). More importantly, we found that bladder cancer cases (Fig. 3E), especially MIBC cases (Supplementary Fig. S4C), with high expression of cytoplasmic DDX31 and high expression of p53 corresponded to a significantly poorer prognosis. Collectively, these findings strongly suggest the possibility that cytoplasmic DDX31 possesses a distinct role in promoting the aggressiveness of bladder cancer.

A tri-complex of DDX31, nucleolin and EGFR regulates EGFR-Akt signaling

To clarify the biological functions of cytoplasmic DDX31 in bladder cancer cells, we focused on nucleolin (NCL), which was previously identified as a candidate interacting partner of DDX31 by analyzing 2-dimensional converted

images of liquid chromatography and mass spectrometry (2DICAL) data (17). Interestingly, recent studies have indicated that NCL is a multifunctional shuttling protein present in the nucleus and cytoplasm and on the surface of some types of cells (24). Hence, we first examined the interaction of DDX31 with NCL by co-immunoprecipitation with anti-DDX31 and anti-NCL antibodies, respectively, and found that DDX31 interacts with endogenous NCL in UM-UC-3 and J82 cells (Fig. 4A and B). Furthermore, accumulating evidence has shown that cytoplasmic NCL interacts with erbB receptors, and especially enhances epidermal growth factor receptors (EGFRs), thereby enhancing EGFR dimerization and activation and promoting EGF ligand-independent cell growth (25, 26). Therefore, we focused on EGFR as a partner of the DDX31-NCL complex and performed immunoprecipitation with an anti-EGFR antibody, followed by Western blot with NCL and DDX31 antibodies. The results showed that endogenous DDX31 interacts with EGFR and NCL in UM-UC-3 cells (Fig. 4C). In addition, we confirmed the endogenous DDX31-NCL interaction in HT1197 (H365R) cells (Supplementary Fig. S5A). More interestingly, we identified a band of high-molecular-weight NCL, which was co-immunoprecipitated with DDX31 and EGFR in cancer cells. Cytoplasmic NCL

was reported to be associated with tumor metastasis of colorectal carcinoma via its phosphorylation status (24). Therefore, to examine whether NCL, which forms a complex with DDX31 and EGFR, is phosphorylated in the cytoplasm of cancer cells, we conducted immunoprecipitation with an anti-DDX31 antibody using nuclear/cytoplasmic fractions of UM-UC-3 cells. As expected, we observed that cytoplasmic DDX31, but not nuclear DDX31, was co-immunoprecipitated with EGFR and phosphorylated NCL (T76/T84), which was reported to play a role in tumor progression (24), in cancer cells (Fig. 4D). Next, we examined the knockdown effect of DDX31 and NCL on EGFR-Akt signaling in UM-UC-3 and found that depletion of DDX31, but not NCL, led to significant attenuation of EGFR protein (Fig. 4E, left and Supplementary Fig. S5B) but did not mRNA (Fig. 4E, right), thereby downregulating Akt (S473) phosphorylation (Fig. 4F). Notably, Kaplan-Meier analysis using the TCGA bladder cancer cohort dataset revealed no significant correlation between *NCL* overexpression and bladder cancer prognosis regardless of p53 mutation status (Supplementary Fig. S5C). Taken together, these findings strongly suggest that cytoplasmic DDX31 may play a crucial role in EGFR stabilization via its binding to phospho-NCL, thereby

promoting EGF ligand-independent constitutive activation of EGFR-Akt signaling and resulting in enhanced progression of p53-mutated MIBC cells.

Development of DDX31-peptide targeting DDX31-NCL interaction

We demonstrated the crucial role of a tri-complex of DDX31, NCL and EGFR in bladder cancer progression, and strategies to inhibit DDX31-NCL may represent potential bladder cancer therapies. To determine the DDX31 region(s) required for interaction with NCL through biochemical analysis, we first independently co-transfected six partial constructs of HA-tagged DDX31 (Fig. 5A) with FLAG-tagged NCL into HEK293T cells. Immunoprecipitation with an anti-FLAG antibody indicated that FLAG-NCL strongly co-immunoprecipitated with $DDX31_{1\text{-}827}$, $DDX31_{1\text{-}783}$, $DDX31_{750\text{-}851}$ and full-length $DDX31_{1\text{-}851}$ and weakly co-immunoprecipitated with $DDX31_{1\text{-}765}$ but not with $DDX31_{1\text{-}750}$, suggesting that amino acid residues 751-765 of DDX31 are directly required for its interaction (Fig. 5B).

We next examined the possibility of a cell-permeable dominant negative peptide targeting the DDX31-NCL interaction and designed a specific peptide (DDX31-peptide) that included the potential NCL-binding region target for the

DDX31-NCL interaction (750-RDAPRNLSALTRKKR-764) and membrane-permeable polyarginine residues (11R) at its NH_2 terminus (Fig. 5C). Immunoprecipitation experiments using an anti-DDX31 antibody revealed that that DDX31-peptide attenuated the tri-complex formation of NCL, EGFR and DDX31 in both UM-UC-3 and J82 cells (Fig. 5D). We further examined the effect of the DDX31-peptide on EGFR-Akt signaling because activation of EGFR-Akt signaling is involved in the invasive behavior of bladder cancer cells (27). The results showed that DDX31-peptide led to a decrease in EGFR protein and Akt phosphorylation levels but not NCL and DDX31 protein levels in UM-UC-3 cells (Fig. 5E), suggesting that DDX31-peptide induced downregulation of EGFR-Akt signaling via its inhibition of the DDX31-NCL interaction. Furthermore, we examined the knockdown effect of DDX31 expression on signaling pathways including pFOXO1/3, mTOR, pS6, p4EBP1 as targets outside of EGFR-Akt pathway in bladder cancer cells, and found that DDX31-depletion resulted in remarkable downregulation of pFOXO1/3, mTOR, pS6, p4EBP1 as well as pAkt phosphorylations in UM-UC-3 cells (Supplementary Fig. S6), suggesting the possibility that DDX31 regulates mTOR-S6/p4EBP1 and pFOXO1/3 as

EGFR-Akt-downstream targets via its interaction with EGFR and NCL in bladder cancer cells.

Furthermore, we noticed that DDX31-peptide treatment led to a much greater increase in nuclear DDX31 protein levels, whereas it caused a decrease in cytoplasmic DDX31 levels in cancer cells (Fig. 6A). Accordingly, we hypothesized that activation of Akt signaling is required for the shuttling of DDX31 between the nucleus and cytoplasm and examined the distribution of DDX31 in cancer cells under activation of Akt signaling by EGF stimulation. The results showed that EGF stimulation led to a remarkable increase in cytoplasmic DDX31 in a dose-dependent manner in UM-UC-3 and J82 cells (Fig. 6B), whereas DDX31-peptide inhibited all phosphorylation of EGFR (Y1068) and Akt (S473) even in the presence of EGF stimulation (Fig. 6C). These findings suggest the possibility that activation of Akt signaling may be involved in the translocation of DDX31 from the nucleus to the cytoplasm. To further clarify this possibility, we treated UM-UC-3 cells with the Akt-specific inhibitor MK-2206 and found attenuation of cytoplasmic DDX31 but increased nuclear DDX31 (Fig. 6D). Collectively, these findings suggest that Akt signaling may be required for the

shuttling of DDX31 between the nucleus and the cytoplasm of bladder cancer cells.

Antitumoral effects of DDX31-peptide targeting DDX31-NCL interactions

As we demonstrated a critical role of the DDX31-NCL-EGFR tri-complex in the progression of bladder cancer in cases bearing *TP53* mutations, we next elucidated the inhibitory effect of DDX31-peptide on spheroid formation by using UM-UC-3-GFP cells. Treatment with DDX31-peptide, but not a control-peptide (717-733 residues of DDX31: Fig. 5C), significantly reduced spheroid formation in a dose-dependent manner (Fig. 7A). In addition, DDX31-peptide, but not the control-peptide, suppressed invasion of UM-UC-3-GFP cells even in the presence of EGF-stimulation (Fig. 7B), suggesting that the DDX31-peptide potentially inhibited the progression of cancer, such as invasion and anchorage-independent growth, regardless of EGF stimulation.

To determine the anti-tumoral effect of DDX31-peptide *in vivo*, UM-UC-3 xenografts were developed in nude mice. Once the tumors were fully established, DDX31-peptide (3.6 and 7.2 mg/kg) and PBS (-) as a control were administered daily by intraperitoneal injection for 25 days. DDX31-peptide

induced significant inhibition of tumor growth in a dose-dependent manner compared to mice treated with PBS (-) (Fig. 7C and Supplementary Fig. S7A). No toxicity or significant body weight changes were observed in either xenograft throughout these experiments (Supplementary Fig. S7B). To clarify the mechanism of the *in vivo* anti-tumoral effect of DDX31-peptide, we first examined its effect on EGFR-Akt signaling. Western blot analysis showed that a significant reduction of EGFR protein expression levels was evident in tumors treated with both concentrations (3.6 and 7.2 mg/kg) of DDX31-peptide compared to those treated with PBS (-) (Fig. 7D). Subsequent immunohistochemical staining analysis also confirmed that EGFR expression and Akt phosphorylation levels were clearly reduced in tumors treated with 3.6 mg/kg or 7.2 mg/kg DDX31-peptide compared with tumors treated with PBS (-) (Fig. 7E). Taken together, these results suggest that DDX31-peptide targeting DDX31-NCL interactions acts as an effective therapeutic drug against advanced invasive bladder cancers.

DISCUSSION

Mutation of the *TP53* gene and EGFR activation have been frequently reported in bladder carcinoma; however, it remains unclear how each alteration contributes to the malignant evolution of bladder cancer. In this study, we present evidence of dual crucial roles of DDX31 in the multistep progression of MIBC with mutated *TP53*. First, we demonstrated that nuclear DDX31 forms a ternary transcriptional complex with mutp53-SP1, thereby enhancing its transcriptional activity and upregulating the target gene *EPB41L4B* and resulting in increased migration and invasion of bladder cancer. *EPB41L4B* belongs to the FERM (4.1, ezrin, radixin and moesin) protein family and is involved in membrane–cytoskeletal interactions and has been shown to promote cancer metastasis in melanoma, prostate cancer and breast cancer (21). Furthermore, analysis of TCGA revealed that MIBC cases with *DDX31* overexpression and bearing mutp53 corresponded to a much poorer prognosis than cases bearing only mutp53. These findings strongly suggest that the cooperation of DDX31 with mutp53 is essential for invasion and migration of MIBC cells (Fig. 7F). Importantly, in more advanced MIBC cases bearing mutp53, cytoplasmic DDX31 forms a complex with EGFR via its interaction with phosho-nucleolin (NCL), thereby contributed to EGFR stabilization and leading to constitutive activation of

EGFR-Akt signaling (Fig. 7F). Collectively, these findings suggest that nuclear and cytoplasmic DDX31 overexpression are critical events in the multistep progression of invasive bladder cancer.

Furthermore, we demonstrated here that NPM1, SP1 and all types of mutp53 bound to 700-749, 541-699 and 611-699 amino acids of DDX31, respectively (Supplementary Fig. S8A-F). More importantly, regarding the anti-proliferative effect, treatment with DDX31-peptide specifically inhibit the DDX31-NCL interaction, but not inhibit the interaction of DDX31 with other binding partners such as NPM1, mutp53 and SP1 (Supplementary Fig. S8G), thereby suppressing EGFR-Akt signaling activation, resulting in suppression of the aggressiveness of MIBC *in vitro* and *in vivo* (Fig. 7F, right square).

Our previous study showed that DDX31 binds to NPM1 in the nucleoli, thereby preventing NPM1–HDM2 complex formation and the subsequent enhancement of HDM2-mediated wild-type p53 ubiquitination and degradation in RCC cells (17).

Furthermore, we here demonstrated for the first time that DDX31 directly interacts with the mutp53-SP1 transcriptional complex and regulates the increase in mutp53 transcriptional activation in bladder cancer cells. Notably,

DDX31 interacts with all types of mutp53 in bladder cancer cell lines, in addition to hotspot mutations (R175H, R248W, R273H and R282W), where it localizes at the DNA binding domain with lost tumor suppressive activity of the wild-type p53 gene, thereby enhancing the transcriptional activation of mutp53. Intriguingly, DDX31 also bound to mutp53 protein with a nonsense mutation within the oligomerization domain in TCCSUP cells (E349X). Accordingly, the DDX31-binding region is conserved in these mutp53, indicating that these mutations has no effect on its transcriptional or SP1 binding activities, leading to possible enhancement of mutp53 GOF activities.

The exact mechanisms underlying the nucleocytoplasmic shuttling of DDX31 that leads to its binding to mutp53 in the nucleus and EGFR-NCL in the cytoplasm of bladder cancer cells remain to be elucidated. We demonstrated that EGF-stimulation induced increased cytoplasmic DDX31, which binds to the EGF-NCL complex (Fig. 6B), whereas the DDX31-peptide led to decreased cytoplasmic DDX31, but increased nuclear DDX31 in cancer cells (Fig. 6A). Notably, treatment with DDX31-peptide led to suppression of EGF-dependent EGFR-Akt signaling activation. Accordingly, we propose the possibility that Akt activation is a crucial event for shuttling DDX31 between the nucleus and

cytoplasm. Moreover, in addition to mutated *TP53*, PTEN inactivation/Akt signaling activation are also critical events for invasive bladder tumors (28). Hence, we hypothesized that EGF-independent Akt signaling activation via loss of PTEN is a trigger of nucleocytoplasmic DDX31 shuttling in bladder cancer cells because PTEN loss occurs owing to Akt activation. Interestingly, analysis of TCGA cohort data provided evidence supporting this hypothesis: MIBC patients bearing mutated *TP53*/high *DDX31* expression/Akt phosphorylation or *PTEN* loss had a significantly worse prognosis than other patients (Supplementary Fig. S9A and B). To clarify this hypothesis, we examined the effect of Akt inhibition on DDX31 shuttling between the nucleus and cytoplasm and found that treatment with the Akt-specific inhibitor MK-2206 led to attenuation of cytoplasmic DDX31 but an increase in nuclear DDX31 in UM-UC-3 cells with loss of *PTEN* (Fig. 6D). Collectively, these findings suggest that Akt activation is a common key event for the transport of DDX31 from the nucleus to the cytoplasm of cancer cells, although further analyses are necessary to confirm this effect.

Most importantly, from a therapeutic point of view, we demonstrated the *in vivo* anti-tumoral effect of DDX31-peptide targeting the DDX31-NCL

interaction. As expected, considering the adverse effects in mice that received high doses of DDX31-peptide (7.4 mg/kg) daily for 25 days, no obvious morphological changes were observed likely because DDX31 is only minimally detectable in normal human organs. However, in fact, the inhibitory effect on DDX31-NCL interaction by DDX31-peptide was not completed (Fig. 5D). Therefore, it is necessary to determine the crucial regions or amino acids required for the DDX13-NCL interaction and to improve the pharmacologic properties of DDX31 using chemical synthetic approaches. Furthermore, MIBC patients who both overexpressed DDX31 and exhibited high p53 expression (mutation) exhibited a much poorer prognosis. Our findings indicate that the combination of DDX31 overexpression and p53 positivity may be a prognostic biomarker for bladder cancer progression.

In conclusion, DDX31 overexpression is critical for the progression of MIBC via its association with mutp53 and EGFR. More importantly, inhibition of the DDX31-NCL interaction represents a potential new treatment avenue for MIBC patients. This new approach targeting DDX31 could be an important supplemental therapy and diagnosis and might provide mechanistic insight into the molecular basis of MIBC.

Acknowledgements

We greatly thank Ms. Hinako Koseki and Ms. Hitomi Kawakami for providing excellent technical supports, and Dr. Osamu Ogawa (Department of Urology, Kyoto University, Kyoto, Japan) and Dr. Bert Vogelstein (Johns Hopkins University) for giving the RT112 RCC and HCT116 p53 (-/-) cell lines, respectively. This study was supported by Scientific Support Programs for Cancer Research, Grant-in-Aid for Scientific Research on Innovative Area (Dr. Takashi Tokino, Department of Medical Genome Sciences, Research Institute for Frontier Medicine, Sapporo Medical University School of Medicine, Sapporo, Japan), a grant/research support from Grants-in-Aid for Scientific Research (B) (MEXT KAKENHI Grant Number 25293079 and16H05153 to T. Katagiri) and a Grants-in-Aid for Scientific Research on Innovative Areas (MEXT KAKENHI Grant Number 16H01575 to T. Katagiri). We would like to thank Springer Nature Author (authorservices.springernature.com) Services for the English language review.

REFERENCES

1. Antoni S, Ferlay J, Soerjomataram I, Znaor A, Jemal A, Bray F. Bladder

Cancer Incidence and Mortality: A Global Overview and Recent Trends. Eur Urol 2017;71:96-108.

2. Witjes JA, Comperat E, Cowan NC, De Santis M, Gakis G, Lebret T, et al. EAU guidelines on muscle-invasive and metastatic bladder cancer: summary of the 2013 guidelines. Eur Urol 2014;65:778-92.
3. Bellmunt J, Petrylak DP. New therapeutic challenges in advanced bladder cancer. Semin Oncol 2012;39:598-607.
4. Vogelstein B, Lane D, Levine AJ. Surfing the p53 network. Nature 2000;408:307-10.
5. Brown CJ, Lain S, Verma CS, Fersht AR, Lane DP. Awakening guardian angels: drugging the p53 pathway. Nat Rev Cancer 2009;9(12):862-73.
6. Xu J, Wang J, Hu Y, Qian J, Xu B, Chen H, et al. Unequal prognostic potentials of p53 gain-of-function mutations in human cancers associate with drug-metabolizing activity. Cell Death Dis 2014;5:e1108.
7. Muller PA, Vousden KH. Mutant p53 in cancer: new functions and therapeutic opportunities. Cancer Cell 2014;25:304-17.
8. Mak AS. p53 in cell invasion, podosomes, and invadopodia. Cell Adhesion & Migration 2014;8:205-14.

9. Freed-Pastor WA, Mizuno H, Zhao X, Langerod A, Moon SH, Rodriguez-Barrueco R, et al. Mutant p53 disrupts mammary tissue architecture via the mevalonate pathway. Cell 2012;148:244-58.

10. Do PM, Varanasi L, Fan S, Li C, Kubacka I, Newman V, et al. Mutant p53 cooperates with ETS2 to promote etoposide resistance. Genes Dev 2012;26(8):830-45.

11. Girardini JE, Napoli M, Piazza S, Rustighi A, Marotta C, Radaelli E, et al. A Pin1/mutant p53 axis promotes aggressiveness in breast cancer. Cancer Cell 2011;20:79-91.

12. Nicholson RI, Gee JM, Harper ME. EGFR and cancer prognosis. Eur J Cancer 2001;37 Suppl 4:S9-15.

13. Rebouissou S, Bernard-Pierrot I, de Reynies A, Lepage ML, Krucker C, Chapeaublanc E, et al. EGFR as a potential therapeutic target for a subset of muscle-invasive bladder cancers presenting a basal-like phenotype. Sci Transl Med 2014;6:244ra91.

14. Takata R, Katagiri T, Kanehira M, Tsunoda T, Shuin T, Miki T, et al. Predicting response to methotrexate, vinblastine, doxorubicin, and cisplatin neoadjuvant chemotherapy for bladder cancers through genome-wide gene

expression profiling. Clin Cancer Res 2005;11:2625-36.

15. Uehara H, Kim SJ, Karashima T, Shepherd DL, Fan D, Tsan R, et al. Effects of blocking platelet-derived growth factor-receptor signaling in a mouse model of experimental prostate cancer bone metastases. J Natl Cancer Inst 2003;95:458-70.

16. Pinto JA, Araujo J, Cardenas NK, Morante Z, Doimi F, Vidaurre T, et al. A prognostic signature based on three-genes expression in triple-negative breast tumours with residual disease. NPJ Genom Med 2016;1:15015

17. Fukawa T, Ono M, Matsuo T, Uehara H, Miki T, Nakamura Y, et al. DDX31 regulates the p53-HDM2 pathway and rRNA gene transcription through its interaction with NPM1 in renal cell carcinomas. Cancer Res 2012;72:5867-77.

18. Bieging KT, Mello SS, Attardi LD. Unravelling mechanisms of p53-mediated tumour suppression. Nat Rev Cancer 2014;14:359-70.

19. Cooks T, Pateras IS, Tarcic O, Solomon H, Schetter AJ, Wilder S, et al. Mutant p53 prolongs NF-kappaB activation and promotes chronic inflammation and inflammation-associated colorectal cancer. Cancer Cell 2013;23:634-46.

20. Shimizu K, Nagamachi Y, Tani M, Kimura K, Shiroishi T, Wakana S, et al. Molecular cloning of a novel NF2/ERM/4.1 superfamily gene, ehm2, that is expressed in high-metastatic K1735 murine melanoma cells. Genomics 2000;65:113-20.

21. Bosanquet DC, Ye L, Harding KG, Jiang WG. FERM family proteins and their importance in cellular movements and wound healing (review). Int J Mol Med 2014;34:3-12.

22. Brosh R, Rotter V. When mutants gain new powers: news from the mutant p53 field. Nat Rev Cancer 2009;9:701-13.

23. Sandelin A, Alkema W, Engstrom P, Wasserman WW, Lenhard B. JASPAR: an open-access database for eukaryotic transcription factor binding profiles. Nucleic Acids Res 2004;32(Database issue):D91-4.

24. Wu DM, Zhang P, Liu RY, Sang YX, Zhou C, Xu GC, et al. Phosphorylation and changes in the distribution of nucleolin promote tumor metastasis via the PI3K/Akt pathway in colorectal carcinoma. FEBS Lett 2014;588:1921-9.

25. Di Segni A, Farin K, Pinkas-Kramarski R. Identification of nucleolin as new ErbB receptors- interacting protein. PLoS One 2008;3:e2310.

26. Farin K, Schokoroy S, Haklai R, Cohen-Or I, Elad-Sfadia G, Reyes-Reyes

ME, et al. Oncogenic synergism between ErbB1, nucleolin, and mutant Ras. Cancer Res 2011;71:2140-51.

27. Wallerand H, Cai Y, Wainberg ZA, Garraway I, Lascombe I, Nicolle G, *et al.* Phospho-Akt pathway activation and inhibition depends on N-cadherin or phospho-EGFR expression in invasive human bladder cancer cell lines. Urol Oncol 2010;28:180-8.

28. Knowles MA, Hurst CD. Molecular biology of bladder cancer: new insights into pathogenesis and clinical diversity. Nat Rev Cancer 2015;15:25-41.

FIGURE LEGENDS

Figure 1. DDX31/mutp53 promotes the progression of bladder cancer. **A.** Kaplan–Meier analysis showing the overall survival among bladder cancer patients with respect to *DDX31* expression and *TP53* status using TCGA cohort data (left panel: mutated *TP53*, right panel: wild-type *TP53*). The presence of both high *DDX31* expression and mutated *TP53* was significantly associated with poor overall survival (log-rank test, p=0.038). **B**. Knockdown of DDX31 expression in bladder cancer cell lines UM-UC-3 and J82 as determined by Western blot analysis at 72 and 96 hours after siDDX31 transfection. WT, p53

wild-type; M, p53 mutant. β-actin was used as an internal control. **C.** Invasion of UM-UC-3 and J82 cells that were treated with siDDX31 or siEGFP were assayed using the xCELLigence system. Statistical analysis was performed at 48 hours after start of cell invasion assay using the xCELLigence system. **D.** Validation of the expression of HA-DDX31 stable transfectant-bladder cancer TCCSUP and HT1376 cell lines by Western blot analysis with an HA-tag antibody. siEGFP was used as a negative control. β-actin was used as an internal control. **E.** Invasion of TCCSUP and HT1376 cells transfected with DDX31-HA or an empty vector (Mock) were assayed using the xCELLigence system. Statistical analysis was performed at 48 hours after start of cell invasion assay. **F.** Cell migration ability of UM-UC-3 cells that were transfected with siDDX31 or siEGFP by a wound healing assay. **G.** Spheroid formation assay was performed using UM-UC-3-GFP cells that were transfected with siDDX31 or siLuciferase (siLuc) as a control (upper panel). Representative observation of spheroid formation of siLuc- and siDDX31-transfected cells (lower panels).

Figure 2. DDX31 interacts and enhances mutp53 transcriptional activity. **A.** The endogenous interaction between DDX31 and mutp53 in UM-UC-3, J82 and 5637

cells. Each cell lysate was immunoprecipitated with an anti-DDX31 antibody, followed by immunoblot with an anti-p53 antibody. **B.** The box-plot analysis of *EPB41L4B* expression in patients with bladder cancer with DDX31 expression and mutated or wild-type TP53 using the TCGA data set. ***C.*** Kaplan–Meier survival curves of the overall survival of patients with bladder cancer according to *DDX31* and *EPB41L4B* expression using the TCGA data set. The presence of high expression of both *DDX31* and *EPB41L4B* was significantly associated with poor overall survival (log-rank test, *P*=0.003). **D.** Ternary complex formation among HA-DDX31, mutp53 and SP1. Cell lysate of DDX31-stable transfectant TCCSUP cells was immunoprecipitated with anti-DDX31 (left) or anti-p53 (right) antibodies, followed by immunoblot with the indicated antibodies. **E.** ChIP assays were used to determine the recruitment of DDX31 and mutp53 to the binding sequence within the *EPB41L4B* gene promoter region in TCCSUP cells. **F.** qRT-PCR analysis showing *EPB41L4B* expression in DDX31 or mock-stable transfectant cells transfected with siEGFP or sip53. β-actin was used as an internal control.

Figure 3. Association of DDX31 and p53 positivity with poor prognosis of bladder cancer patients. **A, B.** Representative immunohistochemistry staining of DDX31 (A) and p53 (B) in bladder cancer specimens. **C.** Kaplan–Meier survival curves of cancer-specific survival in patients with bladder cancer according to DDX31 and p53 expression. The presence of high expression of both DDX31 and p53 was significantly associated with poor survival. **D.** Representative immunohistochemistry staining of cytoplasmic DDX31 and nuclear p53 in bladder cancer specimens. **E.** Kaplan–Meier survival curves of cancer-specific survival in patients with bladder cancer according to cytoplasmic DDX31 (cytoDDX31) and p53 expression. The presence of high expression of both cytoDDX31 and p53 was significantly associated with poor survival.

Figure 4. A ternary complex of DDX31, NCL and EGFR. **A, B**. Confirmation of an endogenous interaction between DDX31 and NCL by immunoprecipitation with an anti-DDX31 antibody (A) or an anti-NCL antibody (B) followed by immunoblots with the indicated antibodies in UM-UC-3 and J82 cells. **C.** Confirmation of the endogenous interaction among EGFR, DDX31 and NCL immunoprecipitated with the anti-EGFR antibody followed by immunoblots with

the indicated antibodies in UM-UC-3 cells. **D.** Immunoblot analysis was performed to detect the subcellular localization of EGFR, NCL, phosphor-NCL (T76/T84) and DDX31 after immunoprecipitation with the anti-DDX31 antibody in UM-UC-3 cells. α/β-tubulin (tubulin) and LMNB1 (lamin) were used as loading controls for the cytoplasmic and nuclear fractions, respectively. **E.** Knockdown effect of DDX31 on EGFR expression at the mRNA (lower) and protein (upper) levels in UM-UC-3 cells at 72, 96 and 120 hours after siDDX31 transfection. **F.** Knockdown effect of DDX31 on Akt-phosphorylation (pAkt; S473) in UM-UC-3 cells at 72 hours after siDDX31 transfection.

Figure 5. Development of DDX31-peptide targeting the DDX31-NCL interaction. **A.** A schematic representation of the HA-DDX31 partial deletion constructs is shown. **B.** Immunoblot analyses were performed to identify the NCL-binding region in DDX31. HEK293T cells were transfected with the indicated DDX31 constructs (full-length DDX31, $DDX31_{1–827}$, $DDX31_{1–783}$, $DDX311_{1–765}$, $DDX31_{1\text{-}750}$ and $DDX31_{7501–851}$) and FLAG-NCL. After 48 hours, the cell lysates were immunoprecipitated with an anti-FLAG antibody followed by immunoblotting as indicated. **C.** The DDX31-peptide and control-peptide

sequences are shown. **D.** The inhibitory effects of DDX31-peptide treatment on DDX31–NCL-EGFR complex formations were evaluated in UM-UC-3 (left) and J82 cells (right). Immunoprecipitation with an anti-DDX31-antibody, followed by immunoblots with the indicated antibodies. **E.** Effects of DDX31-peptide treatment on EGFR, NCL and DDX31 protein levels and pAkt (S473) in UM-UC-3 cells at 24 hours after treatment.

Figure 6. The shuttling of DDX31 between the nucleus and cytoplasm of bladder cancer cells. **A.** Effects of DDX31-peptide treatment on subcellular-distribution of DDX31 in UM-UC-3 cells. α/β-tubulin (tubulin) and LMNB1 (lamin) were used as loading controls for the cytoplasmic and nuclear fractions, respectively. **B.** Immunoblot analysis was performed to detect the subcellular localization of DDX31 in the presence of EGF stimulation in J82 and UM-UC-3 cells. α/β-tubulin (tubulin) and LMNB1 (lamin) were used as loading controls for the cytoplasmic and nuclear fractions, respectively. **C.** Effects of DDX31-peptide treatment on EGFR, pEGFR (Y1068), DDX31, Akt and pAkt (S473) in the presence of EGF stimulation in UM-UC-3 cells. β-actin was used as a loading control. **D.** Immunoblot analysis was performed to detect the subcellular localization of

DDX31 in the presence of the Akt-specific inhibitor MK2206. α/β-tubulin (tubulin) and LMNB1 (lamin) were used as loading controls for the cytoplasmic and nuclear fractions, respectively.

Figure 7. Anti-tumoral activity of DDX31-peptide on bladder cancer cells. **A.** Spheroid assay showed anchorage-independent growth inhibitory effects of DDX31-peptide in UM-UC-3 cells. Representative images merged from phase-contrast and green fluorescent channels are shown to demonstrate spheroid formation 144 hours after treatment (left). The spheroid area was calculated as described in CellPLayer™ 96-well kinetic 3D spheroid protocol (Essen Bioscience) (right). **B.** Invasion assay showed anchorage-independent growth inhibitory effects of DDX31-peptide in the presence of EGF stimulation (50 ng/ml) in UM-UC-3-GFP cells. Representative images merged from phase-contrast and green fluorescent channels are shown to demonstrate spheroid formation 72 hours after treatment (left). **C.** The DDX31-peptide inhibited tumor growth in the UM-UC-3 xenograft mouse model. Mice were treated with DDX31-peptide 11 days after injection of UM-UC-3 cells. The tumor volume represents the mean ± SEM of each group (n=6) (right). **D.** Immunoblot

analyses were performed to evaluate the effects of DDX31-peptide, PBS (-) or no treatment on EGFR expression. **E.** Representative HE staining (upper) and immunohistochemical staining of Akt phosphorylation (S473: middle) and EGFR expression (lower) in tumors from xenografts mice treated with DDX31-peptide (3.7 and 7.4 mg/kg) and PBS, respectively. **F.** Crucial roles of DDX31 in multistep progression of TP53 mutated MIBC. In early-stage MIBC, nuclear DDX31 forms a tri-complex with the mutp53-SP1 transcriptional complex, thereby enhancing transcriptional activity and upregulating the target gene *EPB41L4B*, resulting in the promotion of migration and invasion of bladder cancer. In more advanced MIBC cases bearing mutp53, cytoplasmic DDX31 forms a complex with EGFR via its interaction with pNCL, thereby contributing to EGFR stabilization and leading to constitutive activation of EGFR-Akt signaling (left panel). Regarding the anti-proliferative effect, DDX31-peptide treatment led to suppression of EGFR-Akt signaling activation, resulting in suppression of MIBC aggressiveness (right panel).

Figure 1

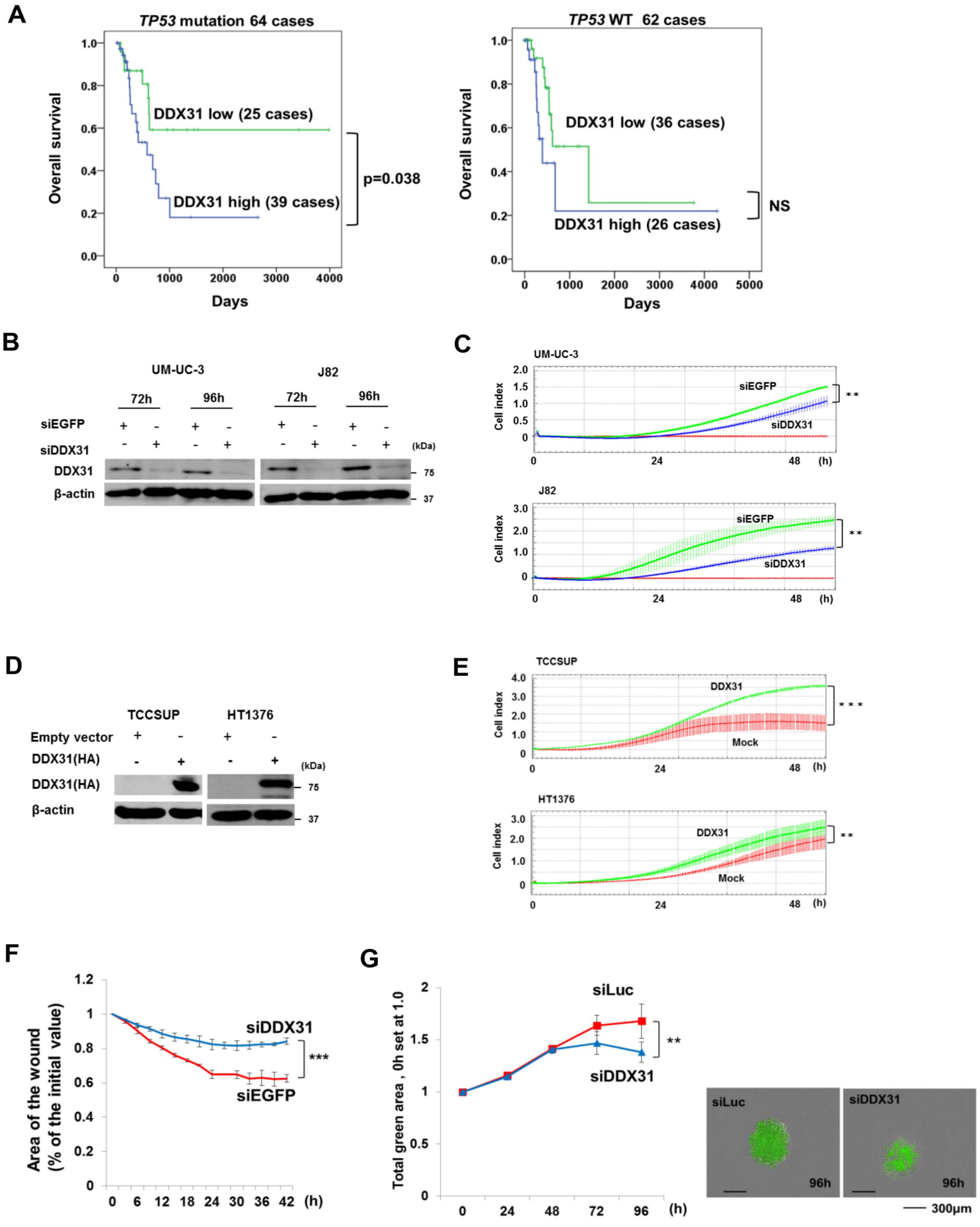

Figure 2

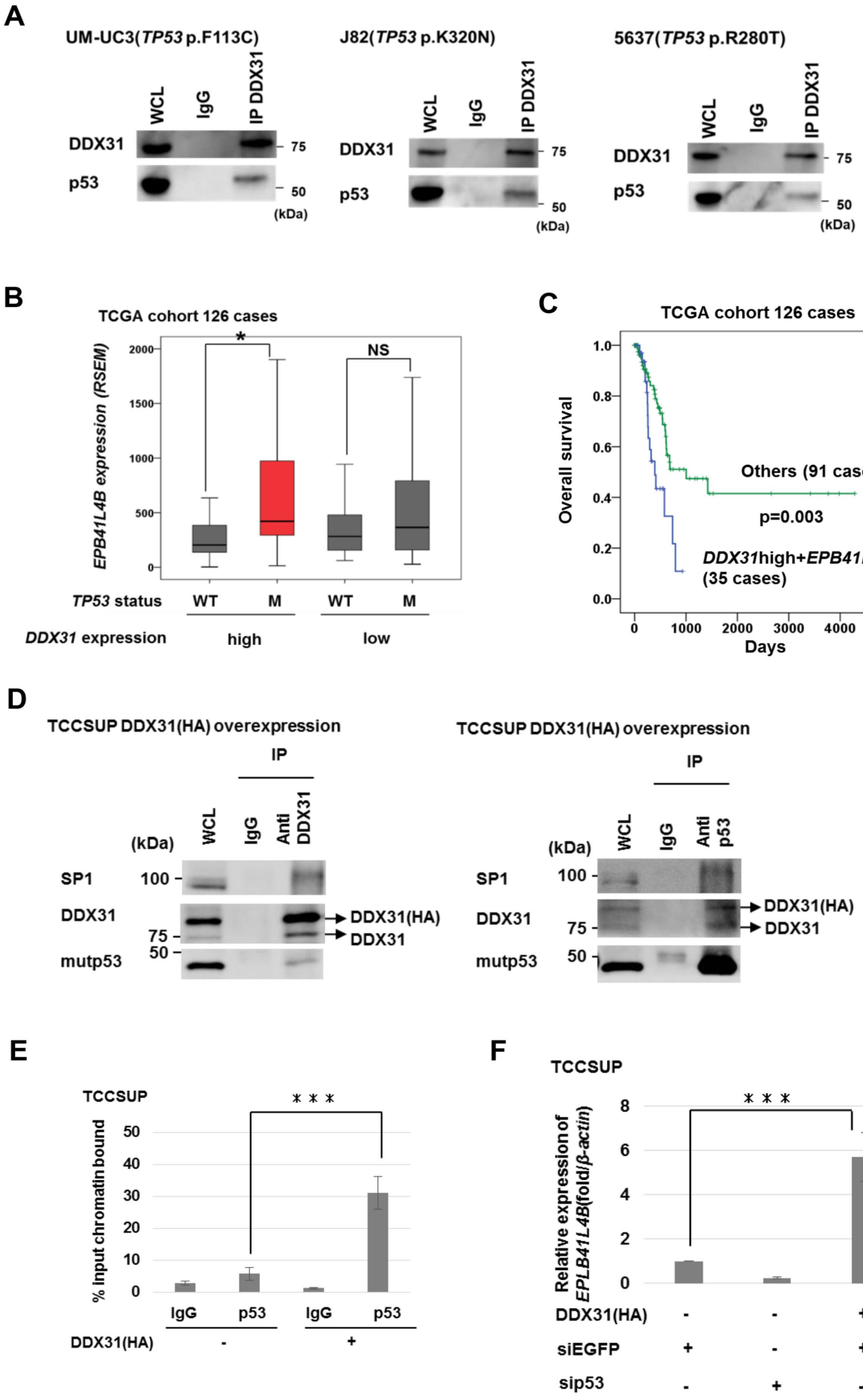

Figure 3

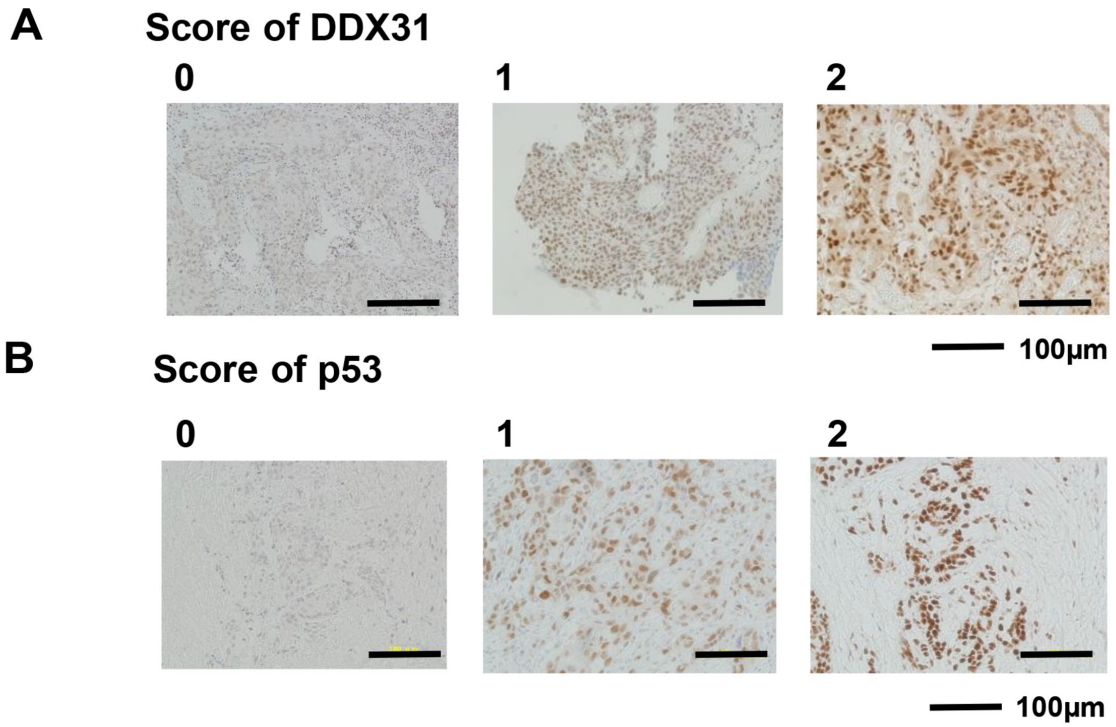

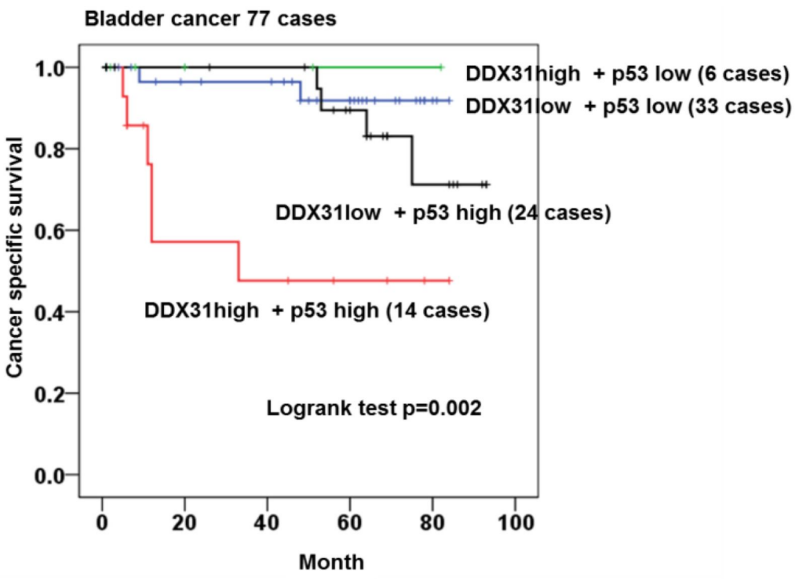

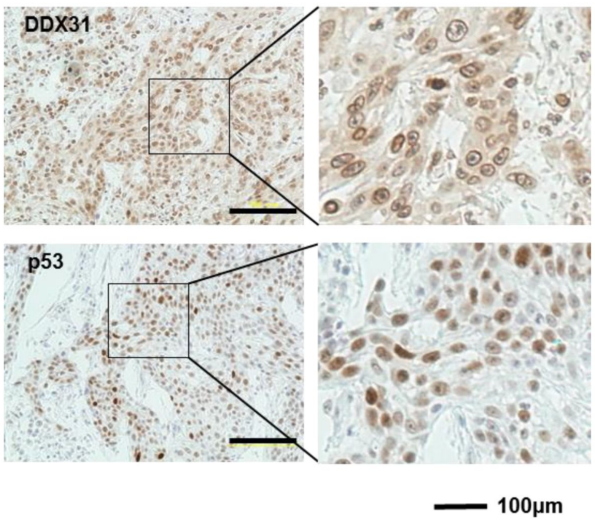

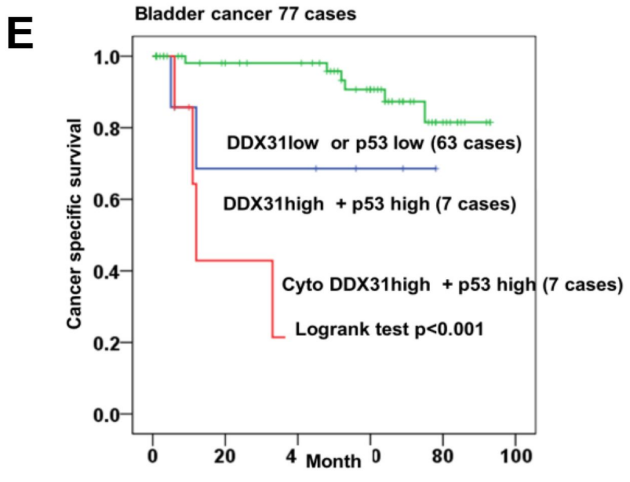

Figure 4

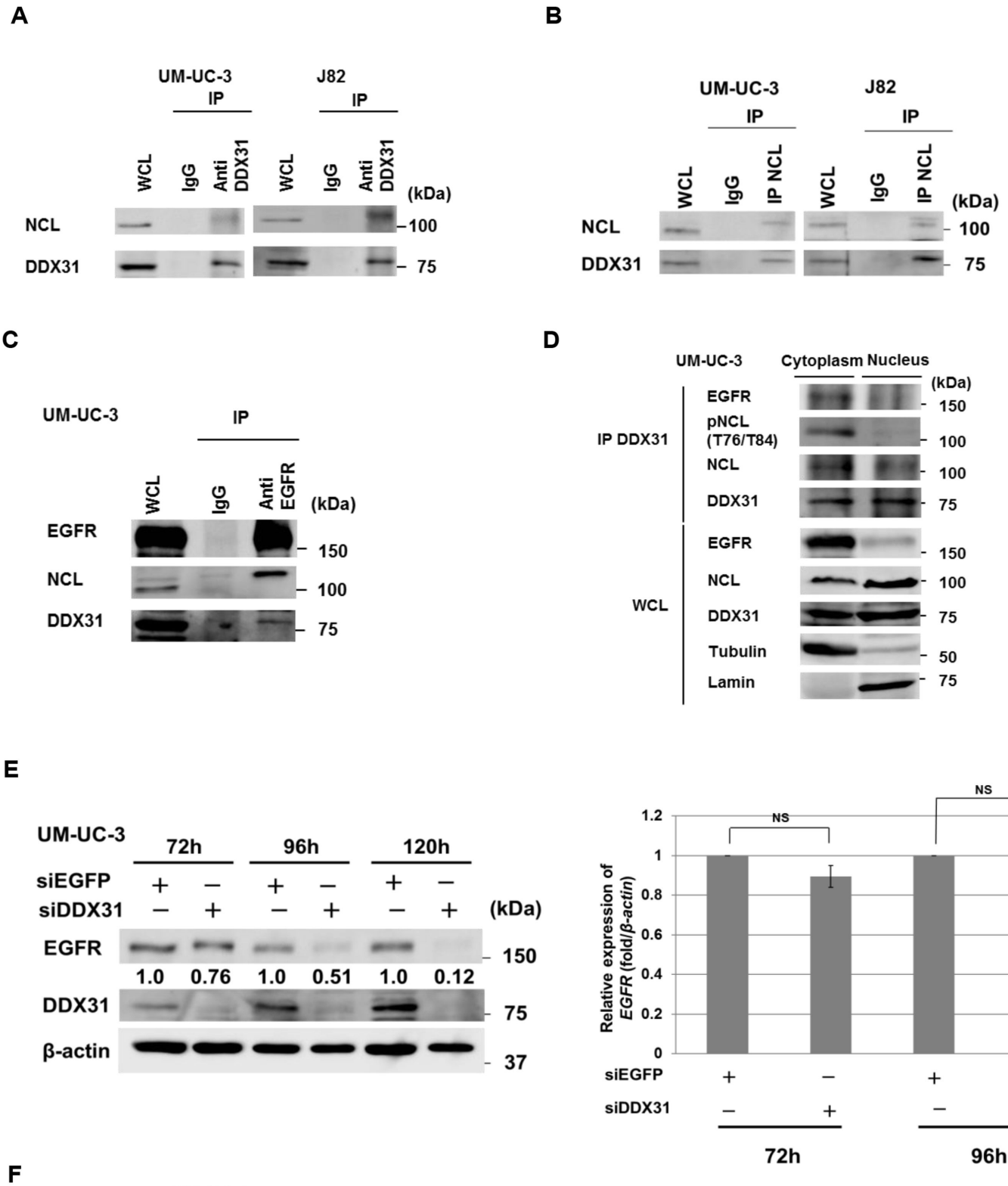

Figure 5

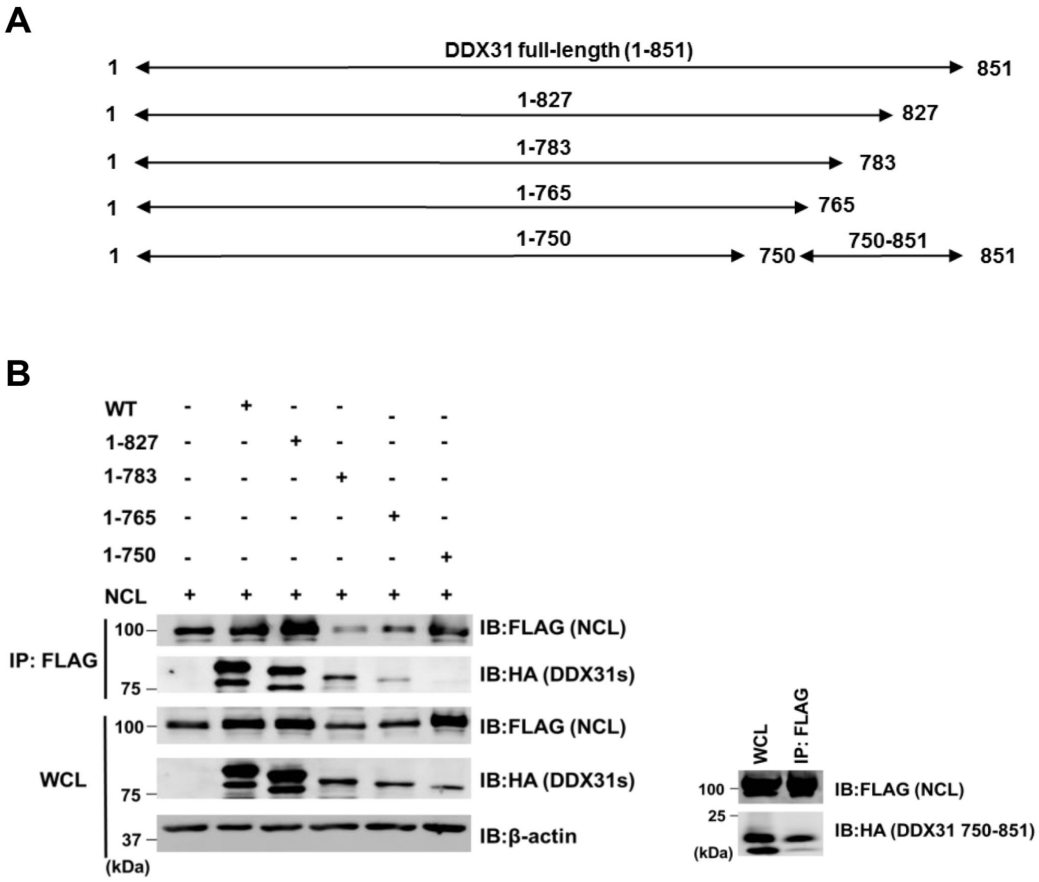

Figure 6

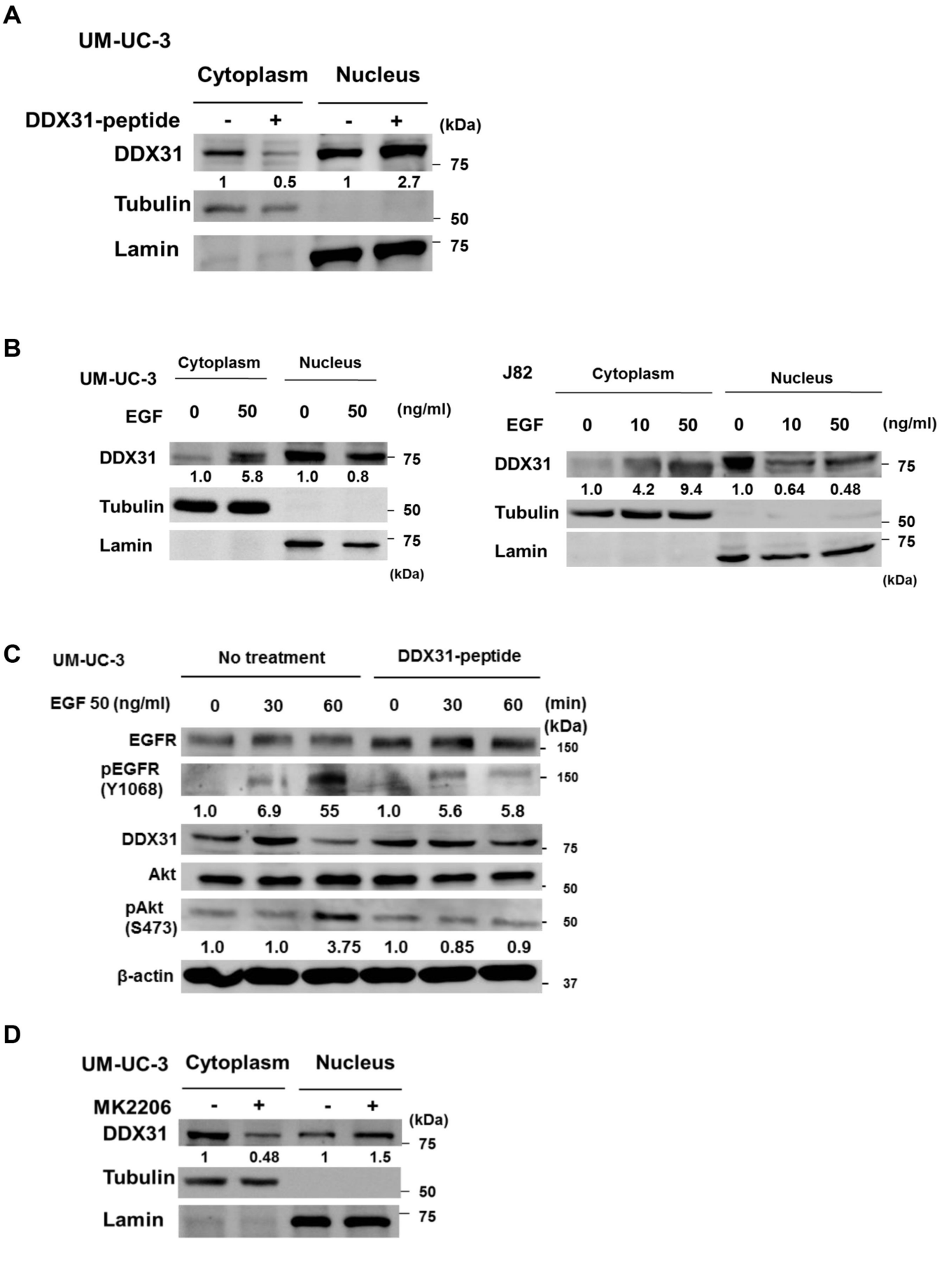

Figure 7

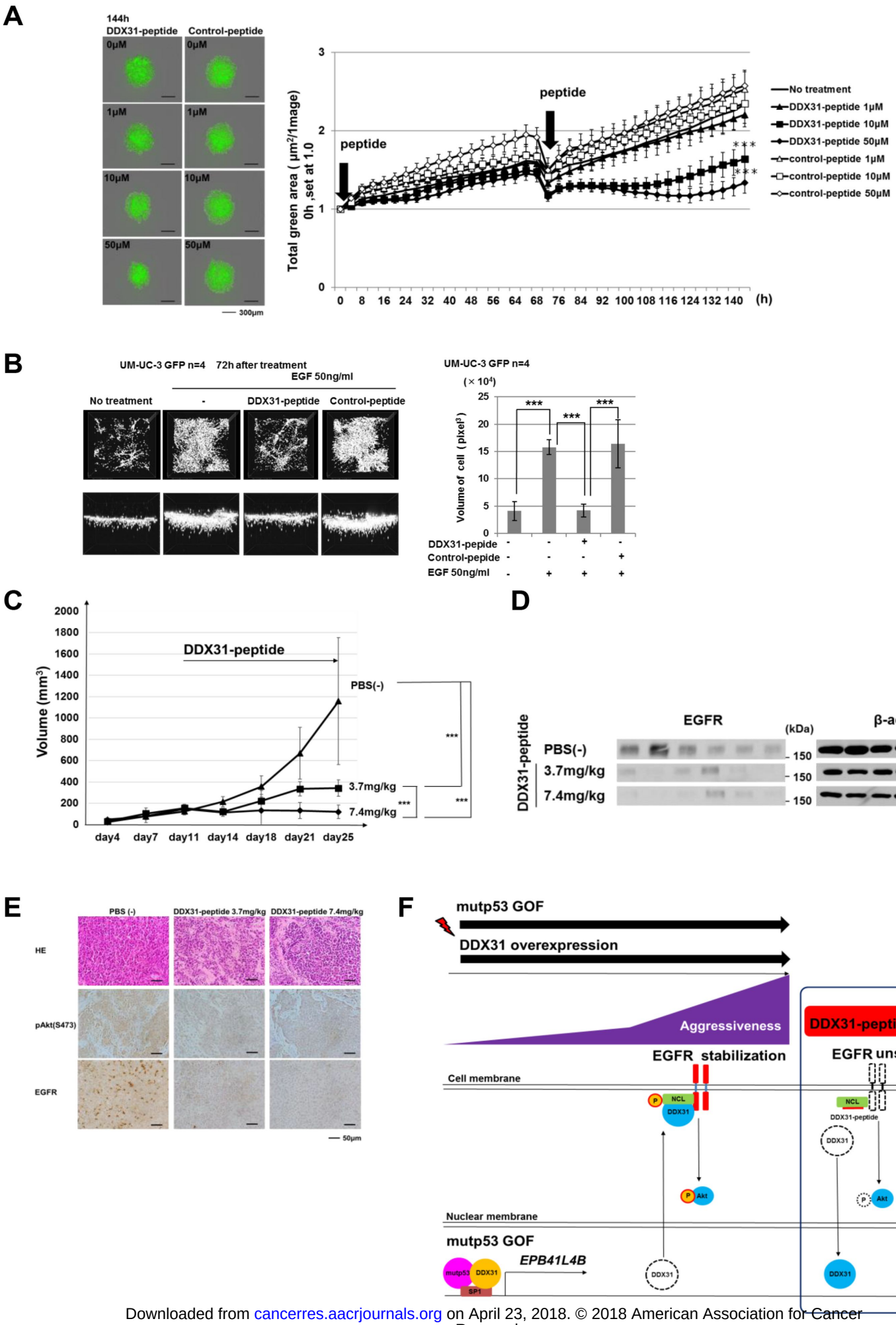

AACR American Association for Cancer Research

Cancer Research

The Journal of Cancer Research (1916–1930) | The American Journal of Cancer (1931–1940)

A DDX31/mutant-p53/EGFR axis promotes multistep progression of muscle invasive bladder cancer

Kei Daizumoto, Tetsuro Yoshimaru, Yosuke Matsushita, et al.

Cancer Res Published OnlineFirst February 13, 2018.